



Pacific Northwest
NATIONAL LABORATORY

Proudly Operated by Battelle Since 1965

Model Test Bed for Evaluating Unstructured-Grid Wave Models for Resource Assessment and Characterization

October 2017

Z Yang
WC Wu
T Wang

DISCLAIMER

This report was prepared as an account of work sponsored by an agency of the United States Government. Neither the United States Government nor any agency thereof, nor Battelle Memorial Institute, nor any of their employees, makes **any warranty, express or implied, or assumes any legal liability or responsibility for the accuracy, completeness, or usefulness of any information, apparatus, product, or process disclosed, or represents that its use would not infringe privately owned rights.** Reference herein to any specific commercial product, process, or service by trade name, trademark, manufacturer, or otherwise does not necessarily constitute or imply its endorsement, recommendation, or favoring by the United States Government or any agency thereof, or Battelle Memorial Institute. The views and opinions of authors expressed herein do not necessarily state or reflect those of the United States Government or any agency thereof.

PACIFIC NORTHWEST NATIONAL LABORATORY
operated by
BATTELLE
for the
UNITED STATES DEPARTMENT OF ENERGY
under Contract DE-AC05-76RL01830

Printed in the United States of America

Available to DOE and DOE contractors from the
Office of Scientific and Technical Information,
P.O. Box 62, Oak Ridge, TN 37831-0062;
ph: (865) 576-8401
fax: (865) 576-5728
email: reports@adonis.osti.gov

Available to the public from the National Technical Information Service
5301 Shawnee Rd., Alexandria, VA 22312
ph: (800) 553-NTIS (6847)
email: orders@ntis.gov <<http://www.ntis.gov/about/form.aspx>>
Online ordering: <http://www.ntis.gov>



This document was printed on recycled paper.

(8/2010)

Model Test Bed for Evaluating Unstructured-Grid Wave Models for Resource Assessment and Characterization

Z Yang
WC Wu
T Wang

October 2017

Coastal Sciences Division
Pacific Northwest National Laboratory

Prepared for
the U.S. Department of Energy
under Contract DE-AC05-76RL01830

Pacific Northwest National Laboratory
Richland, Washington 99352

Summary

Wave resource assessment requires accurate calculation of the wave resource parameters recommended by the International Electrotechnical Commission (IEC) based on high-resolution wave hindcasts. Recent development of unstructured-grid modeling techniques demonstrates the advantages of using unstructured-grid modeling frameworks in simulating wave climates, especially in coastal regions that have complex coastlines, islands, shallow-water bays, and estuaries. The study reported herein evaluated the performance of an unstructured-grid wave model in comparison to a structured-grid model for predicting the IEC wave energy resource parameters at a common test bed site. Model skill was assessed using a set of model performance error statistics. The sensitivity of open boundary conditions and wind forcing on model results, computational efficiency, and the advantages and limitations of the unstructured-grid model were investigated.

This modeling test bed study of wave resource characterization using unstructured-grid wave spectral model SWAN (UNSWAN) on the Level 4 (L4) grids and the extended grids built upon a previous model test bed study (by Sandia National Laboratories [SNL] and Pacific Northwest National Laboratory [PNNL]) of resource characterization that focused on structured-grid wave models. The PNNL study reported herein investigated model performance in simulating the IEC Technical Specification's six recommended wave energy resource parameters—omnidirectional wave power, significant wave height, energy period, spectral width, direction of maximum directionally resolved wave power, and the directionality coefficient—using UNSWAN. It identified the advantages and limitations of unstructured-grid models in comparison to structured-grid models at the same test bed used in the previous joint study by SNL and PNNL.

Model configuration and forcing used in the structured-grid model test bed study were adopted for consistency, and a four-level nested-grid approach—from the global WAVEWATCH III (WWIII) model to the local test bed—was used. All UNSWAN simulations conducted during this study were configured with spectral resolutions of 29 frequency bins and 24 direction bins. Climate Forecast System Reanalysis wind data with 0.5-degree spatial resolution and hourly temporal resolution were used to drive all the model runs.

For all model test cases—WWIII (ST2), UNSWAN (ST2), UNSWAN (ST4), and UNSWAN-EX (ST2)—time series of the six IEC parameters showed good agreement with those calculated from National Data Buoy Center buoy data. The predicted time series for these six parameters from the UNSWAN model, with both ST2 and ST4 physical packages, are comparable to those from the present study's WWIII (ST2) model. This provides confidence in the UNSWAN model settings, although small differences between WWIII and UNSWAN simulations were observed.

The performance of unstructured-grid SWAN on the L4 grid and on the extended grid was investigated. The number of nodes on the L4 grid is nearly two times that of those on the extended grid, but the extended UNSWAN features half of the computational time and more spatial variability for the wave resources assessment. This study demonstrates that unstructured-grid wave modeling provides advantages in computational efficiency and therefore is a practical approach for simulating wave climates near complex geometries that have localized high grid resolution within a large model domain.

Acknowledgments

This study was funded by the U.S. Department of Energy, Office of Energy Efficiency & Renewable Energy, Water Power Technology Office under contract DE-AC05-76RL01830 to Pacific Northwest National Laboratory.

A steering committee, chaired by Bryson Robertson, program manager at the West Coast Wave Initiative, Institute of Energy Systems, at the University of Victoria, was organized to provide external oversight for, input to, and review of this model study. Steering committee members included Prof. Tuba Özkan-Haller, a wave modeling expert at Oregon State University; Dr. Arun Chawla, team lead of the WAVEWATCH III[®] (WWIII) model suite at the National Oceanic and Atmospheric Administration's (NOAA's) National Center for Environmental Prediction; Dr. Brian Polagye, a marine hydrokinetic energy expert at the Northwest National Renewable Energy Center at the University of Washington; Dr. Julie Thomas, program manager and principal investigator for the Coastal Data Information Program from University of California San Diego; Dr. Pukha Lenee-Bluhm, a wave energy expert from Columbia Power; and Mr. Sean Anderton, a manager for technical support from Ocean Renewable Power Company.

Acronyms and Abbreviations

3G	third generation
AWAC	acoustic wave and current (profiler)
CFL	Courant–Friedrichs–Lewis
CFSR	Climate Forecast System Reanalysis
CPU	central processing unit
FVCOM	finite-volume coastal ocean model
GB	gigabyte
GHz	gigahertz
Hz	hertz
IAHR	International Association of Hydraulic Research
IEC	International Electrotechnical Commission
km	kilometer(s)
km ²	square kilometer(s)
kW/m	kilowatt(s) per meter
m	meter(s)
MB	megabyte
MMAB	Marine Modeling and Analysis Branch
MIKE 21	2D hydrodynamic model named after Dr. Mike Abbott
MIKE 21 SW	MIKE 21’s spectral wave module
NDBC	National Data Buoy Center
NCEP	National Centers for Environmental Prediction
NOAA	National Oceanic and Atmospheric Administration
<i>PE</i>	percentage error
<i>RMSE</i>	root-mean-square-error
s	second(s)
<i>SI</i>	scatter index
SSD	solid-state drive
SWAN	Simulating WAves Nearshore
TS	Technical Specification
WAM	WAve prediction Model
WEC	Wave Energy Converter
WWIII	WAVEWATCH III
yr	year(s)

Contents

Summary	iii
Acknowledgments.....	v
Acronyms and Abbreviations	vii
1.0 Introduction	1
2.0 Methods	3
2.1 Test Bed Site and Model Selection	3
2.2 Model Grids	4
2.3 Model Forcing.....	7
3.0 Results and Discussion	9
3.1 Model Simulations	9
3.2 Simulated Wave Resource Parameters.....	9
3.3 Model Performance Metrics.....	11
3.4 Evaluation of Model Skills.....	12
3.5 Computational Requirements.....	21
4.0 Conclusions	23
5.0 References	25

Figures

2.1. Model test bed site off the central Oregon Coast, along with the location of National Oceanic and Atmospheric Administration NDBC 46050 buoy station and the WWIII nested grids.....	4
2.2. Bathymetries of nested grids.....	5
2.3. Unstructured grid of UNSWAN for the test bed and a zoomed-in area in the northwest corner of the domain.....	6
2.4. Extended unstructured grid of UNSWAN for the test bed and a zoomed-in area in the northwest area of the rectangular test bed domain.....	7
2.5. Comparison of CFSR and observed wind speeds at the NDBC 46050 buoy station.....	8
3.1. Comparison of significant wave heights between model simulations using WWIII and UNSWAN with the ST2 physics package and measured data at NDBC 46050 for January–April 2009, May–August 2009, and September–December 2009.....	14
3.2. Comparison of significant wave heights between model simulations using UNSWAN with the ST2 and ST4 physics packages and measured data at NDBC 46050 for January–April 2009, May–August 2009, and September–December 2009.....	15
3.3. Comparison of six UNSWAN (ST2) simulated IEC resource parameters with observed data at NDBC 46050.....	16
3.4. Q-Q plots of six IEC wave resource parameters for UNSWAN using the ST2 physics package.....	17
3.5. Comparison of six UNSWAN (ST4) simulated IEC parameters with observed data at NDBC Buoy 46050.....	18
3.6. Q-Q plots of six IEC wave resource parameters for UNSWAN using the ST2 physics package.....	19

Tables

2.1. WWIII model grids.....	5
2.2. UNSWAN model grids.....	6
3.1. Model run time steps for WWIII (L1–L3 grids) and UNSWAN (L4 grid).....	9
3.2. Performance metrics for WWIII and UNSWAN.....	20
3.3. Performance metrics for UNSWAN runs with different unstructured grids.....	21
3.4. UNSWAN and WWIII computational requirements.....	21

1.0 Introduction

Wave project development relies on consistent and accurate wave resource characterization at a specific site for given feasibility and design classes, as recommended by the International Electrotechnical Commission Technical Specification (IEC TS 2015). The IEC TS also recommends that wave resource characterization be conducted based on six model-simulated wave energy resource parameters using directional wave spectral models. These six resource parameters are omnidirectional wave power, significant wave height, energy period, spectral width, direction of maximum directionally resolved wave power, and the directionality coefficient. Therefore, the accuracy of wave spectral models in simulating wave climate is critical to the success of wave resource characterization, especially in the nearshore region where wave energy deployment is likely to occur. To provide guidance for model selection and modeling best practices for resource characterization, a wave model test bed was established to benchmark, test, and evaluate spectral wave models and modeling methodologies for predicting the wave energy resource parameters recommended by the IEC TS (Neary et al. 2016; Yang et al. 2017). Two of the most widely used structured-grid wave models—WaveWatchIII (WWIII) and Simulating WAVes Nearshore (SWAN) (SWAN Team, 2015)—were evaluated using the nested-grid approach (Neary et al. 2016; Yang et al. 2017). The test bed was selected at a site approximately centered offshore of Newport, Oregon.

Recent development of unstructured-grid wave models demonstrates the advantage of using an unstructured-grid modeling framework in wave modeling, especially in coastal areas that have complex coastlines, islands, shallow-water bays, and estuaries (Qi et al. 2009; Zijlema 2010; Dietrich et al. 2012; Gagnaire-Renou et al. 2012; Robertson et al. 2014; Guillou et al. 2016; Yuk et al. 2016). Therefore, it is necessary to evaluate the performance of unstructured-grid models in comparison to structured-grid models at the same test bed site.

The overall objective of the study reported herein is to evaluate unstructured-grid model skills for predicting the IEC TS's recommended wave energy resource parameters, and to identify the advantage and limitations of unstructured-grid models in comparison to structured-grid models at the same test bed used by Yang et al (2017). Specifically, the following model simulations and analyses were conducted in this study:

- setting up an unstructured-grid model at the wave model test bed site where the structured-grid models WWIII and SWAN were evaluated;
- simulating the IEC TS's six recommended wave energy resource parameters in the wave test bed using a high-resolution unstructured-grid model;
- validating the unstructured-grid modeling using National Data Buoy Center (NDBC) buoy data within the test bed and assessing model skills in comparison to structured-grid models from previous study; and
- evaluating the sensitivity of boundary conditions and wind forcing on model results, computational efficiency, and the advantages and limitations of the unstructured-grid model.

2.0 Methods

Study methods involved test bed site and model selection, model grids, and model forcing, as described in the following subsections.

2.1 Test Bed Site and Model Selection

The same wave test bed site off the central Oregon Coast used in the structured-grid wave model study (Neary et al. 2016; Yang et al. 2017) was adopted in this study. The test bed was selected primarily based on three criteria: 1) high wave energy potential, 2) rich wave data for model validation, and 3) information from previous studies that could be leveraged for this study. Based on the national wave energy resource assessment (EPRI 2011), the central Oregon Coast includes areas of high resource potential where wave power densities range between 35 and 50 kW/m, which can be developed as viable commercial wave energy converter (WEC) projects. The meteorological-ocean (met-ocean) data were collected at real-time NDBC buoy 46050 inside the test bed, which is in the vicinity of a viable commercial WEC location that has representative depth and high-quality, long-term wave measurements. A number of previous studies of wave resource assessment and characterization have been conducted at the test bed site, including the seven-year hindcast data set for the area offshore of Oregon (García-Medina et al. 2014) and the temporal and spatial statistical analysis of the wave resource (Lenee-Bluhm et al. 2011). The test bed site and the location of the NDBC 46050 station are shown in Figure 2.1.

Based on the modeling framework, third-generation (3G) spectral wave models can be divided into two groups: structured-grid and unstructured-grid models. The development of structured-grid wave models has a much longer history than that of unstructured-grid models because of the simple and straightforward discretization of numerical schemes in a structured-grid framework. Popular structured-grid wave models include the Wave prediction Model (WAM; WAMDI Group 1988), WWIII (Tolman 2010; Tolman and WAVEWATCH III 2014) and SWAN (Booij et al. 1999; Rogers et al. 2007; SWAN 2015).

Unstructured-grid models provide advantages in computational efficiency and flexibility for simulating wave climates near complex coastlines. Development of unstructured spectral wave models is new compared to development of structured-grid models. Therefore, applications of unstructured-grid wave models to simulate wave climate and resource characterization are limited. TOMAWAC is a 3G spectral wave model within the integrated TELEMAC modeling system that uses finite element numerical methods in an unstructured-grid framework (Gagnaire-Renou et al. 2010). The TELEMAC system was originally developed by the Laboratoire National d'Hydraulique et Environnement in France and primary users were based in European countries. UNSWAN is the unstructured-grid version of SWAN (Zijlema 2010; Cobell et al. 2013; Robertson et al. 2016; Yuk et al. 2016). The main benefit of unstructured grids is that they can be applied to variable spatial meshing with high resolution along complex coastlines and islands. Flexible meshes are also useful for modeling varying water depths that feature sharp gradients. For example, Robertson et al. (2014) applied UNSWAN to simulate wave resource characterization on the Pacific Northwest coast of Vancouver Island in British Columbia, which has very complex coastlines and a narrow continental shelf. MIKE 21 SW is the commercial 3G spectral wave sub-module of the MIKE 21 coastal modeling system that solves the action balance equations on an unstructured grid using a finite-volume method (Sørensen et al. 2004). Similar to UNSWAN, it simulates the effects of various nonlinear physical effects. FVCOM-SWAVE, which is completely based on the same physics of SWAN, is a spectral wave module embedded in the unstructured-grid, finite-volume coastal ocean model (FVCOM) modeling system (Qi et al. 2009; Yang and Wang 2015). An unstructured-grid version of WWIII has been recently developed and is under continuous development and validation (Ardhuin and Roland 2013; Tolman et al. 2014).

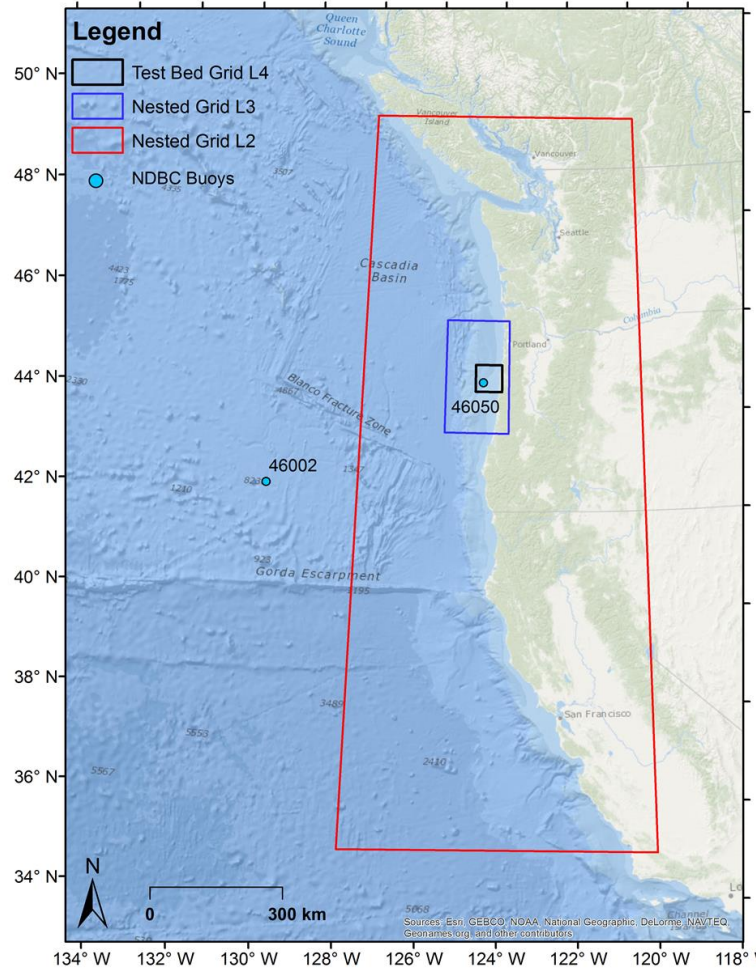


Figure 2.1. Model test bed site off the central Oregon Coast, along with the location of National Oceanic and Atmospheric Administration NDBC 46050 buoy station and the WWIII nested grids.

Based on literature review, UNSWAN and TOMAWAC are more popular and well validated than other unstructured-grid wave models, including MIKE-21 SW, unstructured-grid WWIII, and FVCOM-SWAVE. One drawback of MIKE-21 SW is that it is proprietary software that is not freely available to the public. Therefore, in the initial phase of the unstructured-grid wave model test bed study, UNSWAN was selected based on its maturity and popularity.

2.2 Model Grids

To drive the UNSWAN model for the test bed, a nested-grid modeling approach was employed for the present study. To be consistent with the previous wave test bed study for the structured-grid models, three outer levels of structured-grid WWIII models remain the same as those used in the previous study (Nearby et al. 2016). The level 1 (L1) model is based on the National Oceanic and Atmospheric Administration/ National Centers for Environmental Prediction's (NOAA/NCEP's) global WWIII model with 0.5° grid resolution. The second level (L2) regional grid with a resolution of six arc-minutes was nested into the global model, and the third level (L3) grid with a resolution of one arc-minute, was nested into the regional L2 grid. The model domain coverage (in latitude and longitude), spatial resolution, and grid size

(number of grid points) for the global and the two intermediate nested grids are summarized in Table 2.1. The L3 grid provides open wave boundary conditions for the unstructured-grid test bed model (L4).

Table 2.1. WVIII model grids.

Grid Name	Coverage	Resolution (long., lat.)	Grid size
Global Grid L1	77.5°S - 77.5°N	0.5° × 0.5° (30' × 30')	223,920
Intermediate Grid L2	35° - 50°N; 128° - 120°W	0.1° × 0.1° (6' × 6')	12,231
Intermediate Grid L3	43.6° - 45.9°N; 125.6°-123.8°W	1' × 1'	15,151

Model bathymetry for all grid levels was interpolated from three NOAA bathymetry data sets: the 1 arc-minute ETOPO1 Global Relief Model, the 3 arc-second Coastal Relief Model, and the high-resolution (1/3 arc-second) tsunami bathymetry data. NOAA’s 1 arc-minute ETOPO1 Global Relief Model was used for the outer-shelf region and the deep ocean basins. NOAA’s 3 arc-second (~90 m) Coastal Relief Model for the inner-shelf region was used for the model bathymetry for the L2 to L4 grids. The resolution of the Coastal Relief Model data set is sufficient for the inner-shelf region because the local model grid resolution is ~300 m. The model bathymetry for the test bed domain (L4) was further interpolated from NOAA’s high-resolution (1/3 arc-second) tsunami bathymetry data. The model domain boundaries and bathymetry of the regional and coastal nested grids (L2 and L3) and the test bed site (L4) are shown in Figure 2.2. Figure 2.3 shows the unstructured grid of the test bed site (L4) used by UNSWAN.

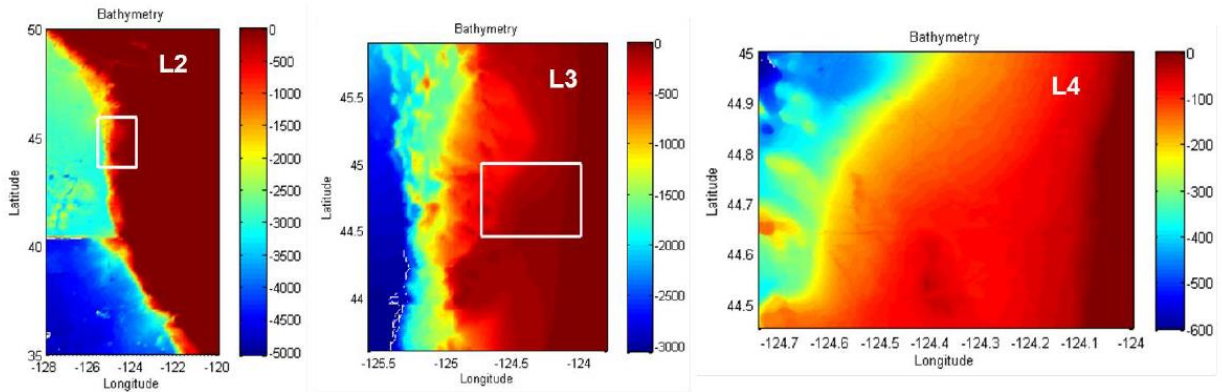


Figure 2.2. Bathymetries of nested grids (L2–L3).

The unstructured grid for the test bed was generated by triangulating the structured grid, which has a dimension of 12 arc-seconds in the longitudinal direction and 10 arc-seconds in the latitudinal direction. The unstructured grid for the L4 domain consists of 44,974 nodes and 89,100 elements (Table 2.2). It should be noted that the unstructured grid generated by directly triangulating the rectangular cell of the structured grid will increase the model resolution in terms of cell/element size.

To demonstrate the flexibility and efficiency of unstructured-grid models, a model simulation with UNSWAN on an extended test bed domain was also conducted. The extended unstructured grid covers a much larger region, from 127°W to 123°W in the longitudinal direction and 42°N to 47°N in the latitudinal direction. The triangle element size inside the test bed domain was specified such that the triangle area is approximately equal to the rectangular area of the structured-grid cell (~ 265 m × 308 m). The extended unstructured grid for the test bed with bathymetry distribution is shown in Figure 2.4 and the grid information is listed in Table 2.2. The average element size of the extended grid inside the test

bed domain is 82,066 m², which is equivalent to a square cell with a length of 286 m and is very close to the rectangular cell size of 265 m × 308 m.

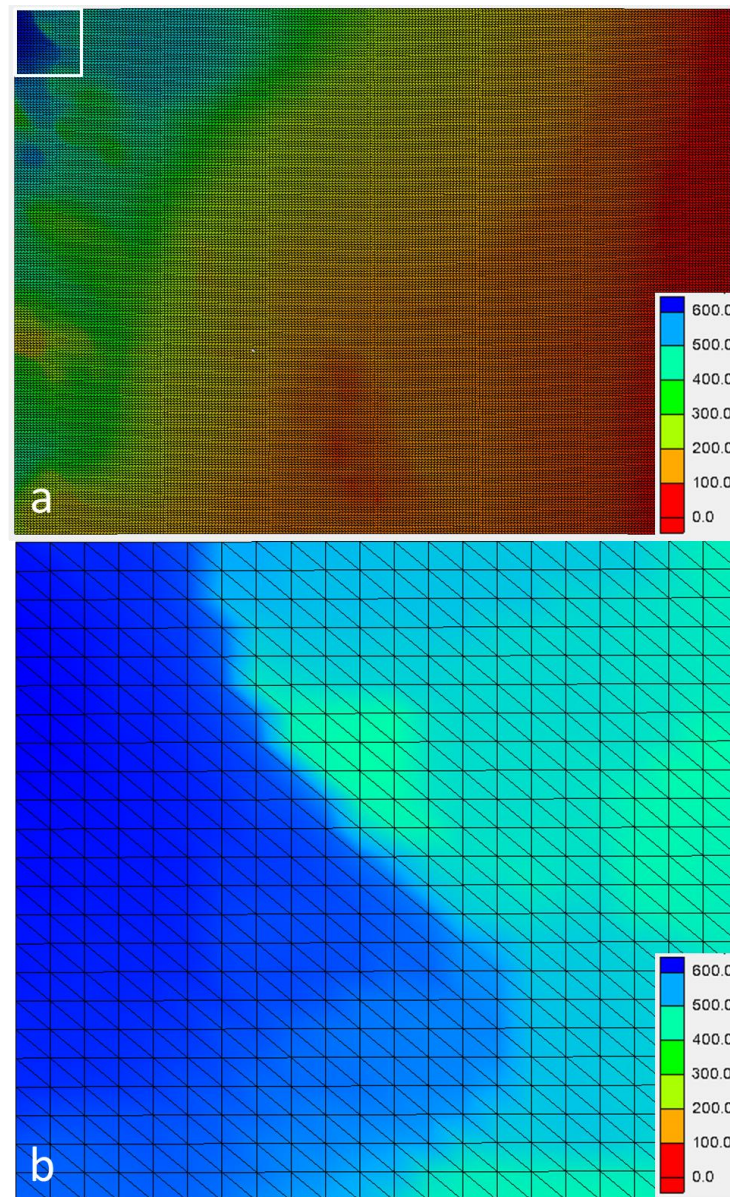


Figure 2.3. Unstructured grid of UNSWAN for the test bed (a) and a zoomed-in area in the northwest corner of the domain (b).

Table 2.2. UNSWAN model grids.

Grid Name	Coverage	Element Size	Node and Element
Test Bed Grid L4	44.45° - 45°N; 124.75° - 124°W	40,540 m ²	(44,974, 89,100)
Extended Test Bed Grid	42° - 47°N; 123° - 127°W	82,066 m ²	(24,107, 47,946)

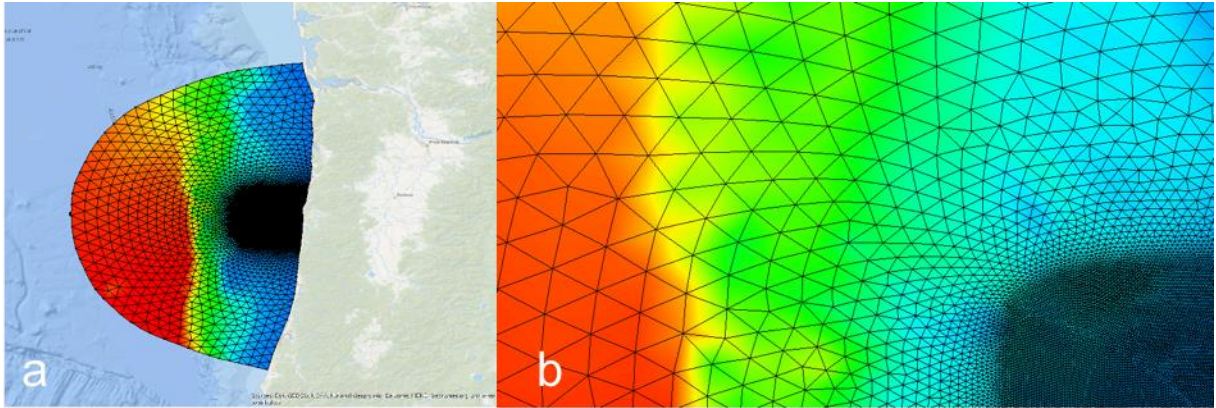


Figure 2.4. Extended unstructured grid of UNSWAN for the test bed (a) and a zoomed-in area in the northwest area of the rectangular test bed domain (b).

2.3 Model Forcing

Sea surface wind forcing is an important factor for accurate simulations of wave growth and dissipation, especially in the nearshore region. In this study, wind speeds and directions were obtained from the Climate Forecast System Reanalysis (CFSR) hindcast simulations and interpolated onto the model grid points. Comparison of CFSR wind speed with observed data at the NDBC 46050 buoy station indicated that the CFSR wind speed is generally in good agreement with the observed speed and reasonably captures the diurnal and seasonal variabilities (Figure 2.5). The CFSR data set meets the minimum 1-hour temporal resolution requirements specified by the IEC TS for design (L3) assessments. However, the 0.5-degree spatial resolution, which is 56 km in the latitudinal direction and 39 km in the longitudinal direction at 45-degree latitude, exceeds the minimum requirements for spatial resolution, which is 25 km for design and 50 km for feasibility. Higher spatial resolution for wind forcing should be considered in the future studies.

The sea ice coverage data were downloaded from the same NCEP CFSR data set as the wind data, except that the original sea ice data were defined in the NCEP T382 Gaussian Grid that has a spatial resolution of 38 km. The sea ice data were subsequently re-projected onto the same 0.5×0.5 degree regular grid as wind forcing and implemented as daily temporal resolution.

Because the test bed site is not close to any estuaries and bays that have strong currents, water surface elevation and currents induced by tides and ocean circulations are not considered in the current study.

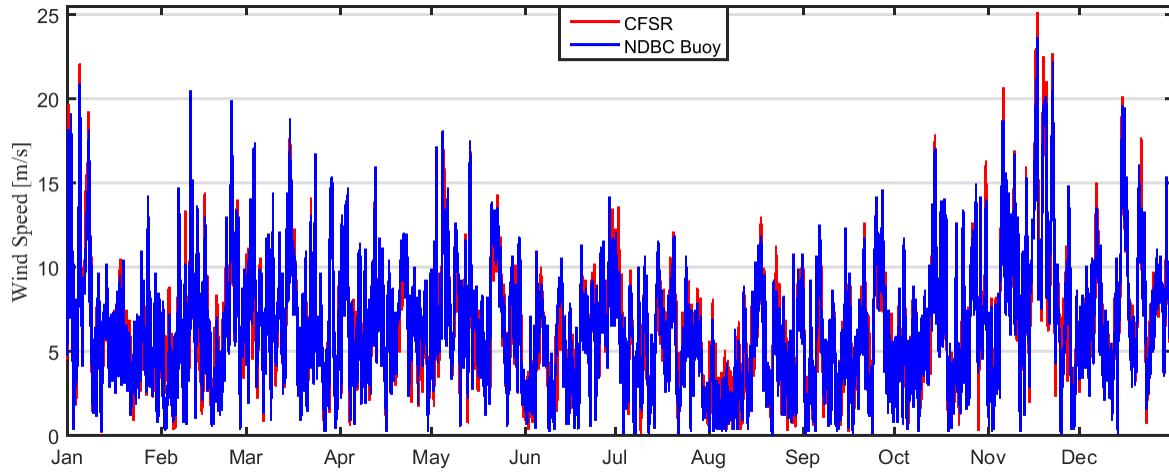


Figure 2.5. Comparison of CFSR and observed wind speeds at the NDBC 46050 buoy station.

3.0 Results and Discussion

The model simulations, wave resource parameters recommended by IEC, model performance metrics, and computational requirements are discussed in the following sections.

3.1 Model Simulations

The model configurations for UNSWAN simulations were specified in the same way as the structured-grid model simulations (Neary et al. 2016). All UNSWAN simulations use 29 frequency bins, 24 direction bins, a logarithmic increment factor of 1.1, a minimum frequency of 0.035 Hz, and a maximum frequency of 0.505 Hz. This spectral resolution meets the minimum requirements specified by IEC TS, i.e., a minimum of 25 frequency components and 24 to 48 directional components, and a frequency range covering at least 0.04 to 0.5 Hz.

Model time steps used in WWIII and SWAN are summarized in Table 3.1. For WWIII, each model grid requires four time steps, the global time step Δt_g , the spatial propagation time step Δt_{xy} , the intra-spectral propagation time step Δt_k , and the source term time step Δt_s (Tolman et al. 2014). The important time step that controls the model stability is the Courant–Friedrichs–Lewis (CFL) time step Δt_{xy} for spatial propagation for the specific model grid resolution.

Table 3.1. Model run time steps for WWIII (L1–L3 grids) and UNSWAN (L4 grid).

WW3 Nested Grid	Δt_g (s)	Δt_{xy} (s)	Δt_k (s)	Δt_s (s)
L1 (global)	3,600	480	1,800	30
L2	600	240	300	15
L3	100	45	50	15
UNSWAN Grid	Δt_{xy} (s)	Input time (s)	Output time (s)	
L4 (test bed)	60	3,600	3,600	

Because the nonstationary UNSWAN model uses an implicit scheme, the computational time step is not restricted by Courant stability criteria. However, the time step does affect the accuracy of the numerical solution. In the present study, a time step of 60 seconds was used for simulations. This time step is more than adequate to resolve the time variations of the computed wave field, given that the wind and open wave boundary forcing inputs are hourly. It was also shown not to affect the accuracy of the numerical solution. Sensitivity studies using smaller time steps, as low as 5 seconds, showed no improvement in the predicted wave parameters.

The calendar year 2009 was selected as the model simulation period based on the availability and completeness of wind forcing data, and met-ocean data for model validation at NDBC 46050. Spectral direction data at NDBC 46050 are available starting from March 5, 2008.

3.2 Simulated Wave Resource Parameters

The six wave resource parameters recommended by IEC TS (2015) were calculated based on model results of directional wave spectra. These six parameters—omnidirectional wave power, significant wave

height, energy period, spectral width, direction of maximum directionally resolved wave power, and directionality coefficient—are defined below.

The omnidirectional wave power, J , is the sum of the contributions to energy flux from each of the components of the wave spectrum,

$$J = \rho g \sum_{i,j} c_{g,i} S_{ij} \Delta f_i \Delta \theta_j \quad (1)$$

where

- ρ = the density of sea water,
- g = the acceleration due to gravity,
- $c_{g,i}$ = the group velocity,
- Δf_i = the frequency bin width at each discrete frequency index i , and
- $\Delta \theta_i$ = the direction bin width at each discrete direction index j .

Directionally unresolved parameters are calculated from one-dimensional (unresolved) frequency variance densities using the equation

$$S_i = \sum_j S_{ij} \Delta \theta_j. \quad (2)$$

For the purpose of the present study the significant wave height is defined as the zeroth frequency of the spectral moment as

$$H_s \sim H_{m0} = 4\sqrt{m_0} \quad (3)$$

where the moments of a variance spectrum are generally defined as

$$m_n = \sum_i f_i^n S_i \Delta f_i. \quad (4)$$

As noted by Tucker and Pitt (2001), this definition of significant wave height was used until 1990 in the United Kingdom when it was defined as the average of the one-third highest zero-crossing waves by the International Association of Hydraulic Research (IAHR 1989). Both definitions give similar results if the distribution of the wave heights fits a Rayleigh distribution.

H_s is typically paired with the energy period, T_e , calculated as

$$T_e = \frac{m_{-1}}{m_0}, \quad (5)$$

to define a wave climate's sea state. The energy period is the variance-weighted mean period of the directionally unresolved variance density spectrum. It is preferred over the peak period, because it is not sensitive to the spectral shape.

The spectral width, ϵ_0

$$\epsilon_0 = \sqrt{\frac{m_0 m_{-2}}{(m_{-1})^2} - 1}, \quad (6)$$

is a measure of the spreading of energy along the wave spectrum. The directionally resolved wave power is the sum of the wave power at each direction θ :

$$J_{\theta} = \rho g \sum_{i,j} c_{g,i} S_{ij} \Delta f_i \Delta \theta_j \cos(\theta - \theta_j) \delta \quad (7)$$

$$\begin{cases} \delta = 1, & \cos(\theta - \theta_j) \geq 0 \\ \delta = 0, & \cos(\theta - \theta_j) < 0 \end{cases}$$

where J_{θ} is the directionally resolved wave power in direction θ . The maximum time-averaged wave power propagating in a single direction, J_{θ_j} , is the maximum value of J_{θ} . The corresponding direction, θ_j , is the direction of maximum directionally resolved wave power and describes the characteristic direction of the sea state.

The directionality coefficient, d , is the ratio of maximum directionally resolved wave power to the omnidirectional wave power,

$$d = \frac{J_{\theta_j \max}}{J} \quad (8)$$

which is a characteristic measure of directional spreading of wave power (i.e., larger values approaching unity signify narrow directional spread).

3.3 Model Performance Metrics

To evaluate the model performance, simulated wave resource parameters are compared to those derived from measurements at NDBC 46050. For each of six wave resource parameters recommended by the IEC TS, the following model performance metrics, commonly used in other modeling studies (e.g., García-Medina et al. 2014; Yang et al. 2017), are computed to quantify the discrepancies between the predicted values derived by model hindcasts and those derived by the NDBC 46050 point measurements. All of these metrics represent an average estimate of the difference between predicted values and measured ones over a defined period of simulation.

The root-mean-square-error (*RMSE*), *aka* root-mean-square-deviation, is defined as

$$RMSE = \sqrt{\frac{\sum_{i=1}^N (P_i - M_i)^2}{N}} \quad (9)$$

where N is the number of observations, M_i is the measured value, and P_i is the predicted value.

RMSE represents the sample standard deviation of the differences between predicted values and measured values.

The percentage error (*PE*) is defined as

$$PE(\%) = \frac{100}{N} \sum_{i=1}^N \left(\frac{P_i - M_i}{M_i} \right) \quad (10)$$

and is the average *PE* over the period of comparison.

The scatter index (SI) is the $RMSE$ normalized by the average of all measured values over the value of comparison, where

$$SI = \frac{RMSE}{\bar{M}}, \quad (11)$$

where the overbar indicates the mean of the measured values.

Model bias, which represents the average difference between the predicted and measured value, is defined as

$$Bias = \frac{1}{N} \sum_{i=1}^N (P_i - M_i). \quad (12)$$

Percentage bias, which is defined as

$$Bias(\%) = \frac{\sum_{i=1}^N P_i - \sum_{i=1}^N M_i}{\sum_{i=1}^N M_i} \cdot 100 \quad (13)$$

is also commonly used to normalize bias.

The linear correlation coefficient, R , is defined as

$$R = \frac{\sum_{i=1}^N (M_i - \bar{M})(P_i - \bar{P})}{\sqrt{(\sum_{i=1}^N (M_i - \bar{M})^2)(\sum_{i=1}^N (P_i - \bar{P})^2)}} \quad (14)$$

and is a measure of the strength of the linear relationship between the predicted and measured values.

3.4 Evaluation of Model Skills

Time series of significant wave heights simulated by UNSWAN with boundary conditions from the WWIII ST2 physics package were compared with measured data at NDBC 46050 in 2009 (Figure 3.1). For reference, model results from WWIII test bed simulations were also plotted in the same figure. Generally, significant wave heights simulated from UNSWAN are very similar to those from WWIII. Model results from UNSWAN show good agreement with observations. UNSWAN was able to reproduce the seasonal variation of the sea state with large waves that occur in the winter and early spring months (November–March) when wind forcing is strong (Figure 2.5), and the calmed sea state during the summer (June–August) when wind forcing is weak. However, both WWIII and UNSWAN tend to under-predict the large waves under some windstorm events during the period from November to March, as shown in Figure 3.1. Figure 3.2 shows the comparisons of measured and modeled significant wave heights from UNSWAN simulations with boundary conditions from WWIII with ST2 and ST4 physics packages. In general, models run with the ST4 physics package slightly improved the significant wave height predictions compared to models run with the ST2 physics package.

The six IEC wave resource parameters were calculated from UNSWAN model results and measured data at NDBC 46050, based on Equations (1–6). Figure 3.3 shows the comparison of six wave resource parameters between UNSWAN model results derived using the ST2 physics package and measured data

for the 2009 period. Overall, model results for all six resource parameters match the measured data well and closely follow the short-term (days) and long-term (months) variations in the measured data, especially for omnidirectional wave power, significant wave height, energy period, and spectral width. In general, the simulated directions of the maximum directionally resolved wave power and directionality coefficients are not as good as the other four parameters. Wave direction parameters are generally more difficult to predict because of the high uncertainty in observed data (NDBC 2009; García-Medina et al. 2014). Model performance was also analyzed by Quantile-Quantile (Q-Q) plots for all six IEC resource parameters (Figure 3.4). The Q-Q plots show good correlations between simulated and observed omnidirectional wave power J , significant wave height H_s , energy period T_e , and spectral width ϵ_0 , similar to time series comparisons (Figure 3.3). However, more scattering in omnidirectional wave power J and significant wave height H_s is observed for large waves, indicating that model skill for predicting large waves under extreme events is not as good as under normal sea state. Correlations for the direction of the maximum directionally resolved wave power and directionality coefficient are not very strong, likely due to the low directional resolution of the model and bias in the observed data, as pointed out by García-Medina et al. (2014).

Comparisons of time series and Q-Q plots of the six IEC resource parameters between simulated results with the ST4 physics package and measured data at the NDBC 46050 buoy are shown in Figure 3.5 and Figure 3.6, respectively. The general patterns of model results using the ST4 physics package are very similar to those using the ST2 physics package (Figure 3.3 and Figure 3.4). However, it can be seen that Q-Q plots for omnidirectional wave power and significant wave height using the ST4 physics package exhibit less scattering for large waves than those using the ST2 physics package.

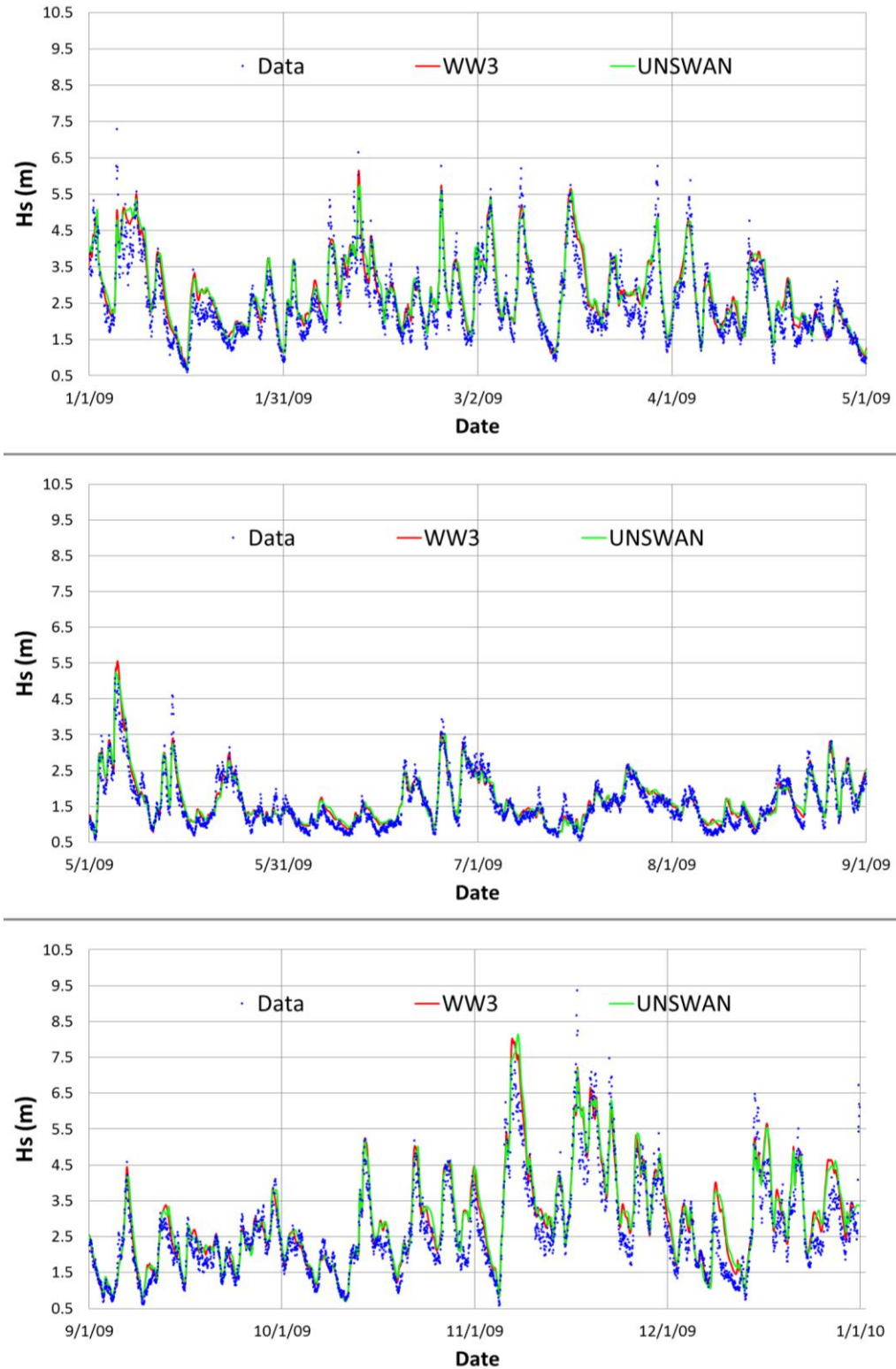


Figure 3.1. Comparison of significant wave heights between model simulations using WWIII and UNSWAN with the ST2 physics package and measured data at NDBC 46050 for a) January–April 2009, b) May–August 2009, and c) September–December 2009.

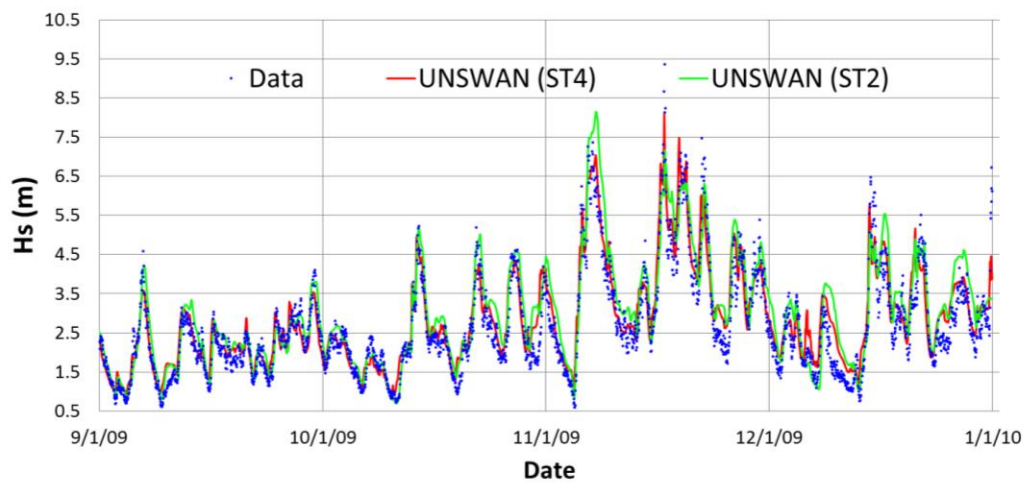
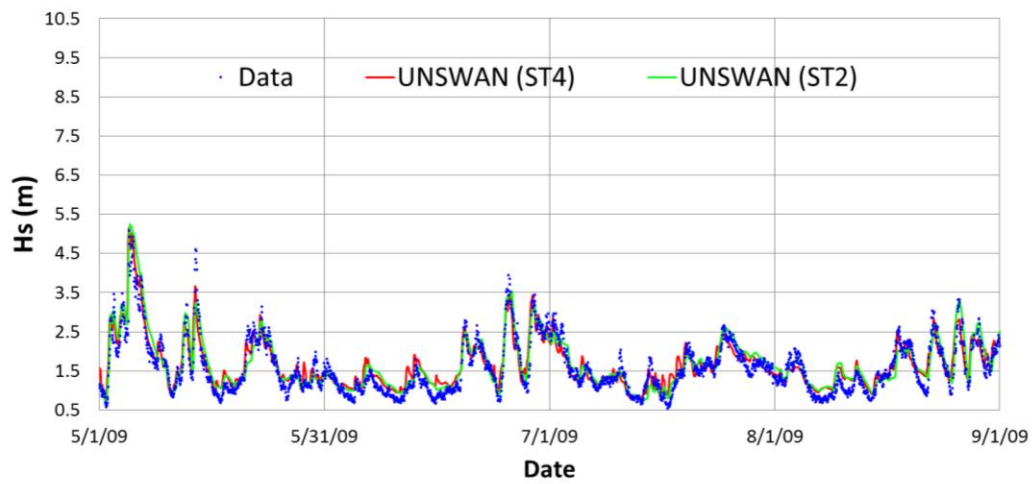
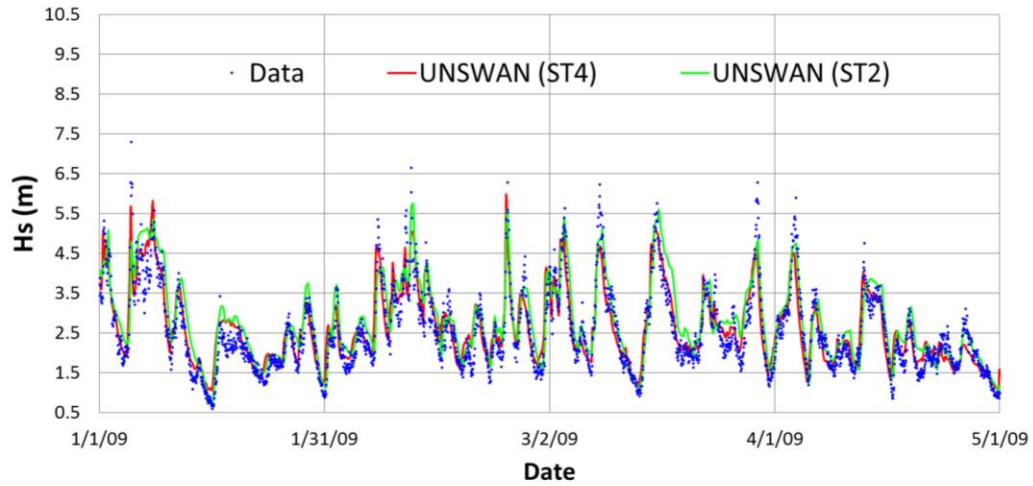


Figure 3.2. Comparison of significant wave heights between model simulations using UNSWAN with the ST2 and ST4 physics packages and measured data at NDBC 46050 for a) January–April 2009, b) May–August 2009, and c) September–December 2009.

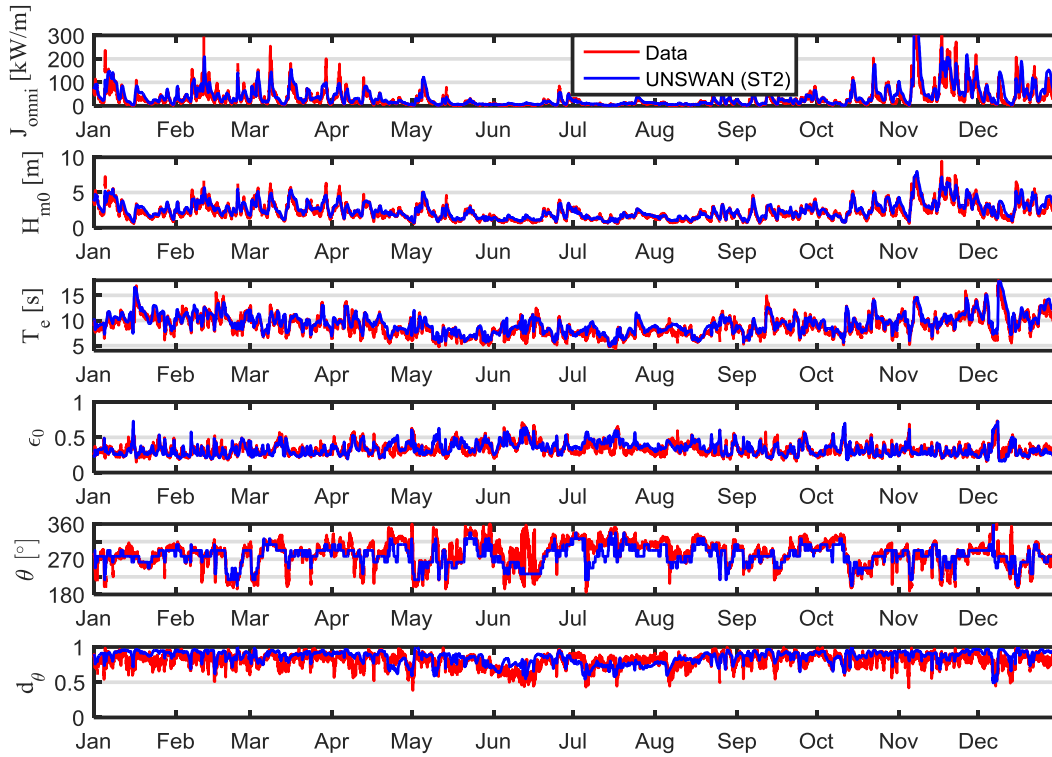


Figure 3.3. Comparison of six UNSWAN (ST2) simulated IEC resource parameters with observed data at NDBC 46050. An open boundary condition is forced with the L3 WWIII model using the ST2 physics package.

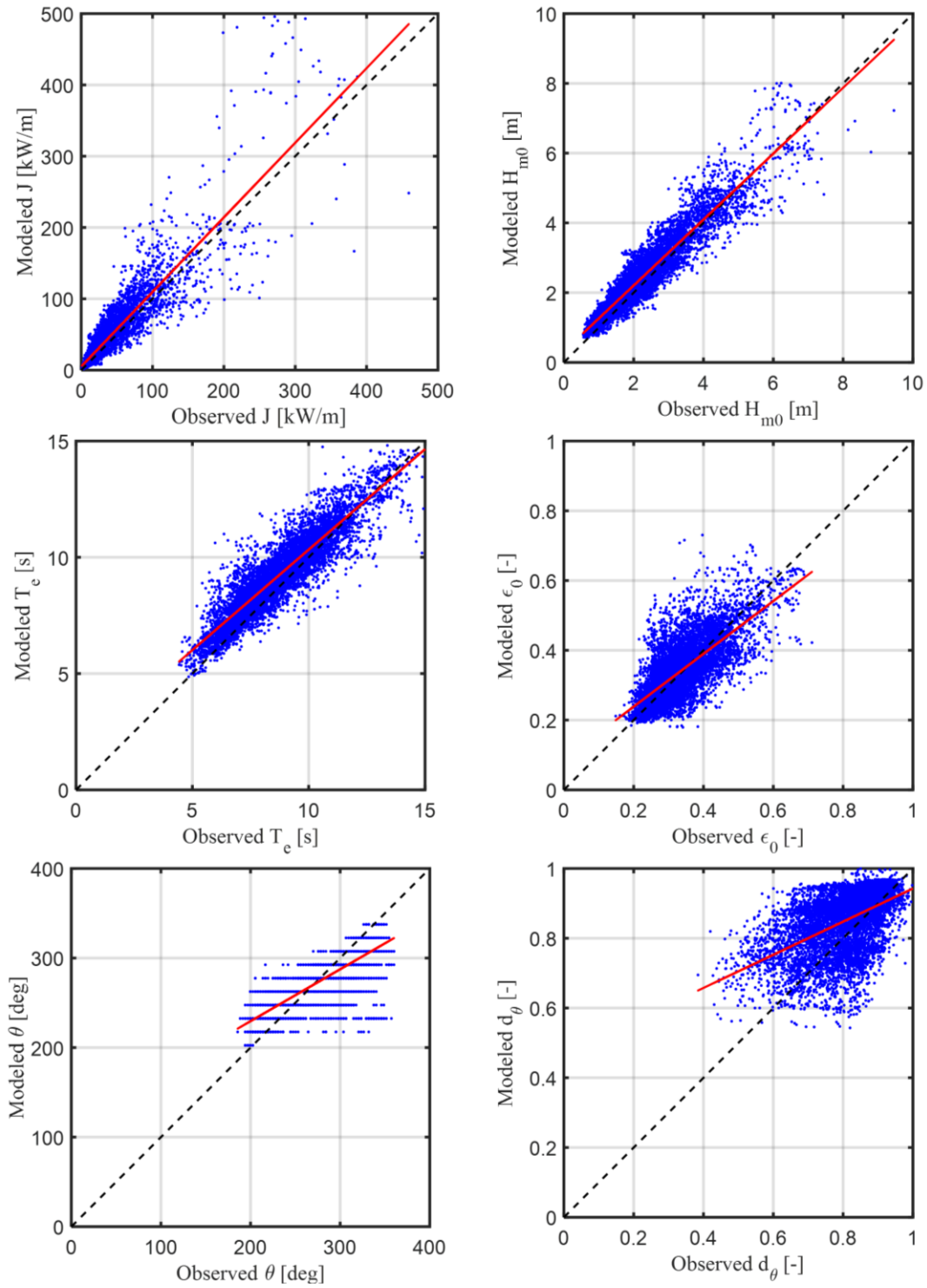


Figure 3.4. Q-Q plots of six IEC wave resource parameters for UNSWAN using the ST2 physics package.

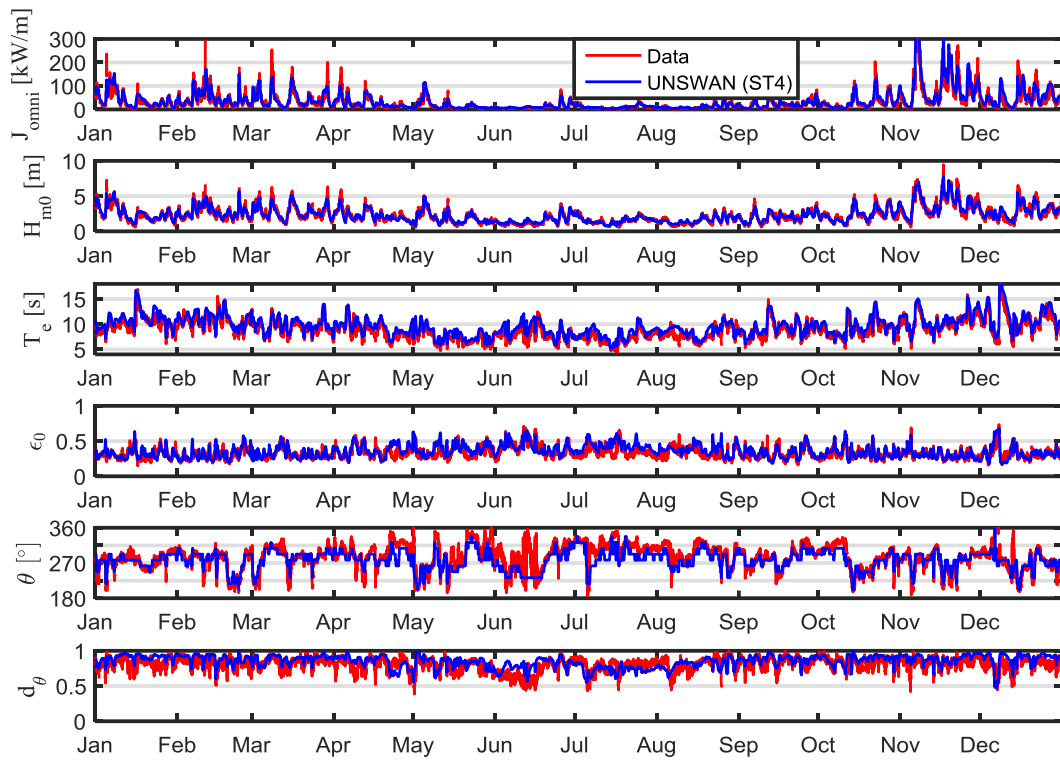


Figure 3.5. Comparison of six UNSWAN (ST4) simulated IEC parameters with observed data at NDBC Buoy 46050. An open boundary condition is forced with the L3 WWIII model using the ST4 physics package.

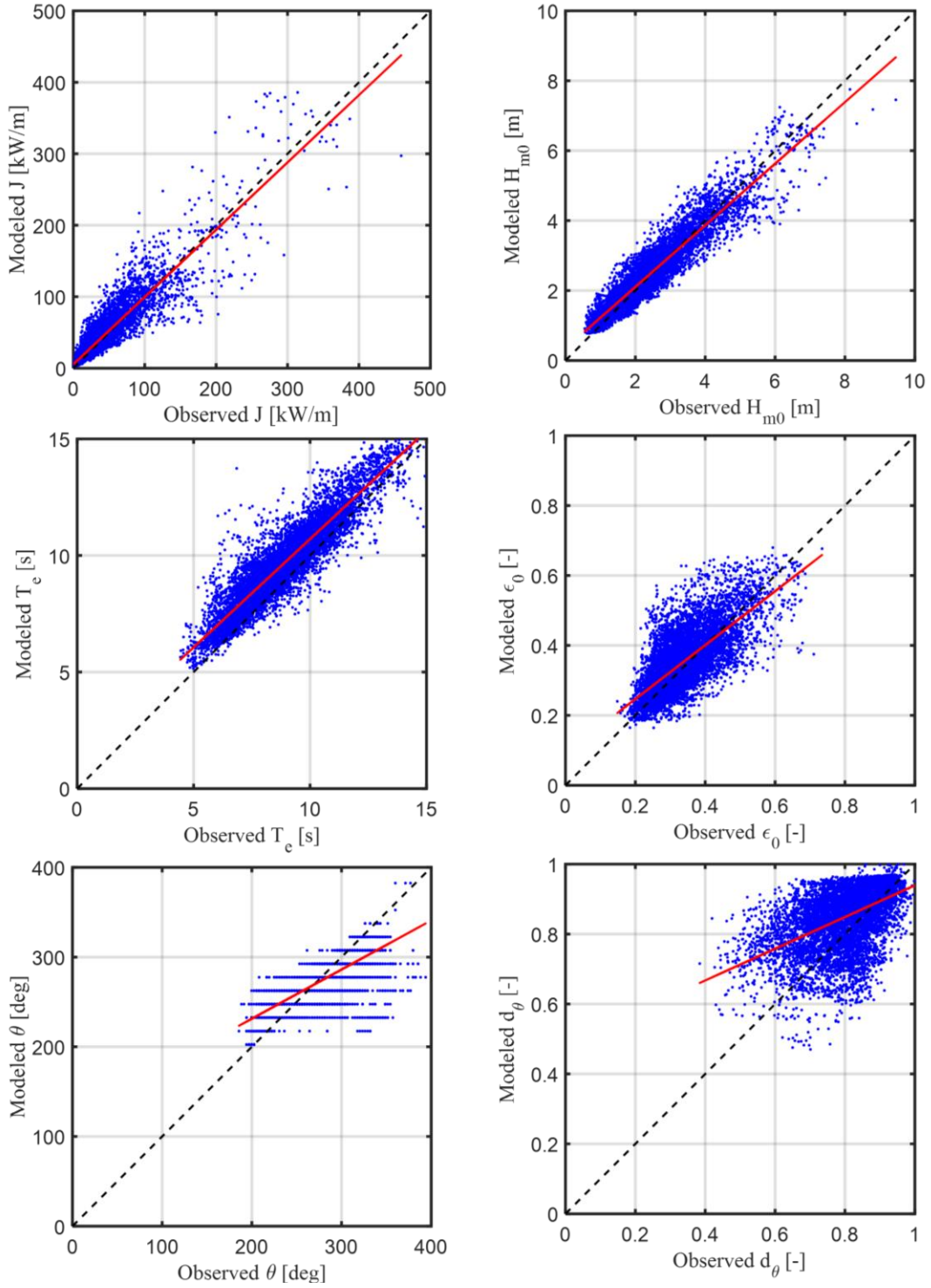


Figure 3.6. Q-Q plots of six IEC wave resource parameters for UNSWAN using the ST4 physics package.

The model performance metrics using WWIII (ST2) and UNSWAN (ST2 and ST4) for each of the six IEC parameters are listed in Table 3.2. WWIII and UNSWAN using the ST2 physics package exhibit similar modeling skills in simulating all six wave resource parameters and the data are in good agreement

with the observed data at NDBC 46050. The correlation coefficients for J , H_s , and T_e with all three model runs are above 0.9. The $RMSE$ for predicted omnidirectional wave power with WWIII (ST2) and UNSWAN (ST2) is 20 (kW/m) and both model runs show bias for over-prediction by approximately 20% (6 kW/m). The PE s for simulated omnidirectional wave power J with WWIII (ST2) and UNSWAN (ST2) are 32% and 38%, respectively. The $RMSE$ for the simulated H_s with WWIII (ST2) and UNSWAN (ST2) is less than 0.5 m and the SI is around 0.20. Both WWIII (ST2) and UNSWAN (ST2) tend to over-predict significant wave height H_s , with a bias of 0.16 m and 0.19 m, respectively. The $RMSE$ s for simulated energy period T_e with both WWIII (ST2) and UNSWAN (ST2) are less than 1.0 s. Similar to wave power and significant wave height, WWIII (ST2) and UNSWAN (ST2) also tend to over-predict wave energy period, with a PE of 6–7% and a bias of 0.5 s. Note that the PE s for omnidirectional wave power are worse than H_s and T_e , because omnidirectional wave power considers wave direction, frequency, and group velocity parameters in its calculation (see Equation [1]). UNSWAN with the ST4 physics package shows better results in simulating the omnidirectional wave power J and the significant wave heights H_s , but slightly worse results in wave energy period T_e (Table 3.2). Error statistics for spectral width ϵ_0 , direction of maximum directionally resolved wave power θ , and directionality coefficient d_θ are similar for all three model runs, as shown in Table 3.2. All three models showed that the simulated ϵ_0 has a $RMSE$ of about 0.06, an SI of 0.2, a PE of less than 6%, a very small bias, and a correlation coefficient of around 0.7. The simulated θ has a $RMSE$ of about 23 degrees, a PE of -2%, and a bias of less than 7 degrees for all three model runs. The simulated directionality coefficient d_θ with all three model runs has a $RMSE$ of 0.1, PE of 6–7%, and bias of 0.04–0.05. The correlation coefficient for the directionality coefficient d_θ is approximately 0.50, much lower than other five resource parameters, as indicated in the Q-Q plots (Figure 3.4 and Figure 3.6).

Comparisons of model performance metrics for the simulated six wave resource parameters with UNSWAN on the L4 grids and the extended grids are provided in Table 3.3. Also, when simulating the six IEC parameters, the extended-grid UNSWAN has performance metrics similar to those of UNSWAN using the L4 grid, even if we use a larger model domain.

Table 3.2. Performance metrics for WWIII and UNSWAN.

Parameter	Model	$RMSE$	PE (%)	SI	Bias	Bias (%)	R
J (kW/m)	WWIII (ST2)	20	32	0.64	6.1	19.7	0.91
	UNSWAN (ST2)	20	38	0.68	6.4	21.4	0.91
	UNSWAN (ST4)	16	32	0.51	3.6	11.5	0.92
H_s (m)	WWIII (ST2)	0.42	9	0.19	0.16	7.3	0.94
	UNSWAN (ST2)	0.44	12	0.20	0.19	8.8	0.94
	UNSWAN (ST4)	0.38	7	0.17	0.07	3.3	0.94
T_e (s)	WWIII (ST2)	0.98	6	0.11	0.50	5.6	0.90
	UNSWAN (ST2)	0.92	7	0.11	0.50	5.7	0.91
	UNSWAN (ST4)	1.10	10	0.12	0.78	8.8	0.92
ϵ_0 (-)	WWIII (ST2)	0.07	3	0.20	0.01	1.6	0.68
	UNSWAN (ST2)	0.06	3	0.19	0.00	1.9	0.72
	UNSWAN (ST4)	0.07	6	0.20	0.02	4.8	0.72
θ (degrees)	WWIII (ST2)	22.87	-2	0.08	-6.87	-2.4	0.74
	UNSWAN (ST2)	21.27	-2	0.07	-6.57	-2.3	0.77
	UNSWAN (ST4)	22.33	-2	0.08	-7.08	-2.5	0.76

Table 4.1. (contd)

Parameter	Model	<i>RMSE</i>	<i>PE</i> (%)	<i>SI</i>	Bias	Bias (%)	R
	WWIII (ST2)	0.10	7	0.13	0.05	6.2	0.48
d_θ (-)	UNSWAN (ST2)	0.10	6	0.12	0.04	5.4	0.53
	UNSWAN (ST4)	0.10	7	0.12	0.04	5.5	0.51

Table 3.3. Performance metrics for UNSWAN runs with different unstructured grids.

Parameter	Model (ST2)	<i>RMSE</i>	<i>PE</i> (%)	<i>SI</i>	Bias	Bias (%)	R
J (kW/m)	UNSWAN	20	38	0.68	6.4	21.4	0.91
	UNSWAN-EX	18	43	0.61	6.0	19.9	0.92
H_s (m)	UNSWAN	0.44	12	0.20	0.19	8.8	0.94
	UNSWAN-EX	0.45	14	0.20	0.20	9.1	0.94
T_e (s)	UNSWAN	0.92	7	0.11	0.50	5.7	0.91
	UNSWAN-EX	0.88	6	0.10	0.45	5.1	0.91
ϵ_0 (-)	UNSWAN	0.06	3	0.19	0.00	1.9	0.72
	UNSWAN-EX	0.06	3	0.19	0.01	2.1	0.72
θ (degrees)	UNSWAN	21.27	-2	0.07	-6.57	-2.3	0.77
	UNSWAN-EX	20.80	-2	0.07	-6.82	-2.4	0.78
d_θ (-)	UNSWAN	0.10	6	0.12	0.04	5.4	0.53
	UNSWAN-EX	0.10	6	0.12	0.04	4.6	0.51

3.5 Computational Requirements

In the present study, all WWIII and UNSWAN simulations were performed in the PNNL Institutional Computing Constance supercomputer. The Constance cluster is a world-class cluster currently composed of 520 dual Intel Haswell-based E5-2670 CPUs (2.3 GHz), providing 24 cores per node. Each node has 64 GB 2133-MHz DDR4 memory and 550 GB local/scratch space on a solid-state drive disk (>450 MB/s speed) and 56Gb/s FDR Infiniband interconnect. Constance ranked 297th on the Top 500 list when initially installed with 300 compute nodes in November 2014.

Computational requirements for WWIII and UNSWAN simulation runs are summarized in Table 3.4. Clearly, WWIII requires significantly more computational resources than UNSWAN. It takes about 5.5 days to complete a 1-year WWIII simulation using 10 nodes (240 cores); while it only takes a few hours for the unstructured-grid SWAN to accomplish the same using the same number of CPUs. Therefore, there is a great advantage to using SWAN for high-resolution wave hindcasts.

Table 3.4. UNSWAN and WWIII computational requirements.

Run ID	Description	CPU-hours
WWIII	ST2, 29×24	31,488
UNSWAN	ST2, 29×24	1,728
UNSWAN-EX	ST2, 29×24	1,152

4.0 Conclusions

After a previous model test bed study for resource characterization that focused on structured-grid wave models (Neary et al. 2016; Yang et al. 2017), a modeling test bed study for wave resource characterization with unstructured-grid wave spectral model SWAN (UNSWAN) on the L4 grids and the extended grids was conducted. The objective of the study was to investigate the model performance in simulating the IEC TS's six recommended wave energy resource parameters using UNSWAN, and to identify the advantages and limitations of unstructured-grid models in comparison to structured-grid models at the same test bed used in the joint study by Sandia National Laboratories and PNNL (Neary et al. 2016). This report summarizes the approach, model results, and study findings.

For consistency, model configuration and forcing used in the structured-grid model test bed study were adopted in the present study. All UNSWAN simulations conducted during the present study were configured with spectral resolutions of 29 frequency bins and 24 direction bins. CFSR wind data with 0.5-degree spatial resolution and hourly temporal resolution were used to drive all the model runs. For all model test cases—WWIII (ST2), UNSWAN (ST2), UNSWAN (ST4), and UNSWAN-EX (ST2)—time series of the six IEC parameters showed good agreement with those calculated from NDBC buoy data. Predicted time series for these six parameters from the UNSWAN model, with both ST2 and ST4 physical packages, are comparable to those from the present study's WWIII (ST2) model. This provides confidence in the UNSWAN model settings, although small differences between WWIII and UNSWAN simulations were observed.

The performance of unstructured-grid SWAN on the L4 grid and on the extended grid was investigated in this study. The performance of both models showed similar results in simulating the wave resource parameters. Also, the number of nodes on the L4 grid is nearly two times that of those on the extended grid, but the extended UNSWAN has half of the computational time and more spatial variability for the wave resources assessment. This study demonstrates that unstructured-grid wave modeling provides advantages in computational efficiency and therefore is a practical approach for simulating wave climates near complex geometries with localized high grid resolution within a large model domain.

5.0 References

- Ardhuin F and A Roland. 2013. The development of spectral wave models: coastal and coupled aspects. In the Proceedings of 7th international Conference on Coastal Dynamics, June 24–28, 2013. Arcachon, France.
- Booij N, RC Ris, and LH Holthuijsen. 1999. A third-generation wave model for coastal regions - 1. Model description and validation. *Journal of Geophysical Research-Oceans* 104:7649–7666.
- Cobell Z, HH Zhao, HJ Roberts, FR Clark, and S Zou. 2013. Surge and Wave Modeling for the Louisiana 2012 Coastal Master Plan. *Journal of Coastal Research* 88–108.
- Dietrich JC, S Tanaka, JJ Westerink, CN Dawson, RA Luetlich, M Zijlema, LH Holthuijsen, JM Smith, LG Westerink, and HJ Westerink. 2012. Performance of the Unstructured-Mesh, SWAN plus ADCIRC Model in Computing Hurricane Waves and Surge. *Journal of Scientific Computing* 52:468–497.
- EPRI (Electric Power Research Institute). 2011. *Mapping and Assessment of the United States Ocean Wave Energy Resource*. EPRI 2011 Technical Report to U.S. Department of Energy, Palo Alto, California.
- Gagnaire-Renou E, M Benoit, and PH Forget. 2010. Ocean wave spectrum properties as derived from quasi-exact computations of nonlinear wave-wave interactions. *Journal of Geophysical Research C (Oceans)* 115, C12, C12058, doi:10.1029/2009JC005665.
- Gagnaire-Renou E, M Benoit, and P Forget. 2012. Spectral wave modeling using a quasi-exact method for nonlinear wave-wave interactions. *Houille Blanche-Revue Internationale De L Eau* :51–60.
- García-Medina G, HT Özkan-Haller, and P Ruggiero. 2014. Wave resource assessment in Oregon and southwest Washington, USA. *Renewable Energy* 64:203–214.
- Guillou N, G Chapalain, and SP Neill. 2016. The influence of waves on the tidal kinetic energy resource at a tidal stream energy site. *Applied Energy* 180:402–415.
- IAHR (International Association of Hydraulic Research). 1989. List of sea-state parameters. *Journal of Waterways, Ports and Ocean Engineering* 115:793–808.
- IEC (International Electrotechnical Commission). 2015. Marine energy – Wave, tidal and other water current converters – Part 101: Wave energy resource assessment and characterization. IEC TS 62600-101. Edition 1.0.2015-06, Geneva, Switzerland.
- Lenee-Bluhm P, R Paasch, and HT Özkan-Haller. 2011. Characterizing the wave energy resource of the US Pacific Northwest. *Renewable Energy* 36:2106–2119.
- NDBC (National Data Buoy Center). 2009. Handbook of automated data quality control checks and procedures. NOAA NDBC Technical Document 09-02; Stennis Space Center, MS.
- Neary VS, Z Yang, T Wang, B Gunawan, AR Dallman. 2016. Evaluating Wave Models and Best Practices for Resource Assessment and Characterization. PNNL- 25385/SAND2016-8497 R, Sandia National Laboratories and Pacific Northwest National Laboratory.

- Qi J, C Chen, RC Beardsley, W Perrie, and G Cowles. 2009. An unstructured-grid finite-volume surface wave model (FVCOM-SWAVE): implementation, validations and applications. *Ocean Modelling* 28:153–166, doi:10.1016/j.ocemod.2009.01.007.
- Robertson B, CE Hiles, and BJ Buckham. 2014. Characterizing the near shore wave energy resource on the west coast of Vancouver Island, Canada. *Renewable Energy* 665–678.
- Robertson B, H Bailey, D Clancy, J Ortiz, and B Buckham. 2016. Influence of wave resource assessment methodology on wave energy production estimates. *Renewable Energy* 86:1145–1160.
- Rogers WE, JM Kaihatu, L Hsu, RE Jensen, JD Dykes, and KT Holland. 2007. Forecasting and hindcasting waves with the SWAN model in the Southern California Bight. *Coastal Engineering* 54:1–15.
- Sørensen OR, Kofoed Hansen H, M Rugbjerg, and LS Sørensen. 2004. A Third Generation Spectral Wave Model Using an Unstructured Finite Volume Technique. In *Proceedings of the 29th International Conference of Coastal Engineering*, 19–24 September 2004, Lisbon, Portugal.
- SWAN Team. 2015. SWAN: User Manual. Delft University of Technology, Environmental Fluid Mechanics Section, available from <http://www.swan.tudelft.nl> (SWAN Cycle III version 41.01A, 2015).
- Tolman HL. 2010. WAVEWATCH III® development best practices. Tech. Note 286, Ver. 0.1, National Oceanic and Atmospheric Administration/National Weather Service/National Centers for Environmental Prediction/Marine Modeling and Analysis Branch, Camp Springs, MD.
- Tolman H and the WAVEWATCH III® Development Group. 2014. User manual and system documentation of WAVEWATCH III® version 4.18. Available from <http://polar.ncep.noaa.gov/waves/wavewatch/> (Version 4.18, 2014).
- Tucker MJ and Pitt EG. 2001. *Waves in Ocean Engineering*. Elsevier Ocean Engineering Book Series, Vol. 5, Elsevier Science Ltd., First Edition.
- WAMDI Group. 1988. The WAM model – a third generation ocean wave prediction model. *Journal of Physical Oceanography* 18:1775–1810.
- Yang Z and T. Wang. 2015. Modeling Wave Resource Characterization - Using an Unstructured-Grid Coastal Ocean Model. In *Proceedings of the 11th European Wave and Tidal Energy Conference*. EWTEC2015, Nantes, France.
- Yang Z, V Neary, T Wang, BT, A Dallman, and WC Wu. 2017. Wave resource modeling test bed study. *Renewable Energy*, 114:132-144. <http://dx.doi.org/10.1016/j.renene.2016.12.057>
- Yuk JH, KO Kim, KT Jung, and BH Choi. 2016. Swell Prediction for the Korean Coast. *Journal of Coastal Research* 32:131–141.
- Zijlema M. 2010. Computation of wind-wave spectra in coastal waters with SWAN on unstructured grids. *Coastal Engineering* 57(3):267–277.



Pacific Northwest
NATIONAL LABORATORY

*Proudly Operated by **Battelle** Since 1965*

902 Battelle Boulevard
P.O. Box 999
Richland, WA 99352
1-888-375-PNNL (7665)

U.S. DEPARTMENT OF
ENERGY

www.pnnl.gov